

# Facile Intermolecular Aryl–F Bond Cleavage in the Presence of Aryl C–H Bonds: Is the $\eta^2$ -Arene Intermediate Bypassed?

Weijun Liu, Kevin Welch, Carl O. Trindle, Michal Sabat, William H. Myers, and W. Dean Harman\*

Department of Chemistry, University of Virginia, Charlottesville, Virginia 22904-4319

Received February 1, 2007

The complex  $\text{TpW}(\text{NO})(\text{PMe}_3)(\eta^2\text{-benzene})$  cleanly inserts into the C–F bond of fluorobenzene to form the seven-coordinate complex  $\text{TpW}(\text{NO})(\text{PMe}_3)(\text{F})(\text{Ph})$  (confirmed by X-ray diffraction), while no C–H insertion is detected. Treatment of this product with triethyl- or phenyldimethylsilane results in liberation of benzene and the corresponding silyl fluoride. DFT calculations suggest a low-energy reaction pathway for C–F activation involving a fluorine-bound  $\sigma$ -complex that does not require the presence of an  $\eta^2$ -arene intermediate. As the fluorine content of the benzene increases, or the benzene is replaced by fluoronaphthalene, C–F addition is no longer observed, and either C–H addition or  $\eta^2$ -coordination dominates. Two species thought to be  $\eta^2$ -silanes are also reported.

## Introduction

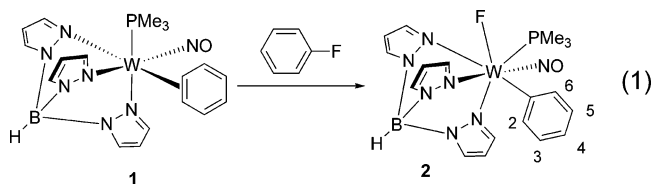
Fluorinated organic compounds are widely used in agrochemicals, pharmaceuticals, refrigerants, plastics, and other applications where chemically inert materials are desired. Consequently, the activation and modification of fluorocarbons by transition metals has been the subject of numerous studies over the past decade.<sup>1–12</sup> Many of these reports have focused on the activation of fluorinated arenes, where the C–F bonds are particularly robust. However, when aryl–hydrogen bonds are also present, C–H activation often dominates.<sup>13–16</sup> Two examples have been reported for the catalytic defluorination of fluorobenzene, but both processes require elevated temperatures and either long reaction times<sup>13</sup> or strongly alkaline conditions.<sup>14</sup>

Transition metal complexes that are known to activate aromatic fluorocarbons include both hydrides (e.g.,  $\text{Cp}^*\text{Rh}(\text{PMe}_3)\text{H}_2$ ,<sup>8</sup>  $\text{Ru}(\text{dmpe})_2\text{H}_2$ ,<sup>15</sup>  $\text{HRh}(\text{PMe}_3)_4$ ,<sup>16</sup> and  $\text{Cp}^*\text{ZrH}_2$ )<sup>4</sup> and non-hydrides (e.g.,  $\{\text{Cp}^*\text{Rh}(\text{PMe}_3)\}$ ,<sup>17</sup>  $\text{Rh}(\text{PMe}_3)_3(\text{SiMe}_2\text{Ph})$ ,<sup>6</sup> and  $\{\text{PEt}_3\}_2\text{Ni}\}$ )<sup>18</sup> examples. For the latter class, activation

occurs by a direct insertion of the metal into a C–F bond. Several reports, bolstered by theoretical calculations, invoke the formation of an  $\eta^2$ -arene intermediate directly preceding this event.<sup>19–21</sup> We speculated that further insight into the C–F activation process could be gained by studying the reactivity of fluoroarenes with the  $\pi$ -base  $\{\text{TpW}(\text{NO})(\text{PMe}_3)\}$ ,<sup>22</sup> a transition metal fragment that has demonstrated a propensity for forming stable  $\eta^2$ -arene complexes and for resisting C–H oxidative addition, despite its highly electron-rich nature.<sup>23</sup>

## Results and Discussion

**1-Fluorobenzene.** The  $\eta^2$ -benzene complex **1**, prepared from the  $\text{W}^{\text{I}}$  precursor  $\text{TpW}(\text{NO})(\text{PMe}_3)\text{Br}$ , is known to readily substitute benzene for other ligands in ether solvents through a largely dissociative mechanism.<sup>23</sup> This complex was dissolved in fluorobenzene, and the solution was allowed to stand overnight at room temperature. Addition of this solution to pentane precipitated compound **2** in 78% yield (eq 1).



Spectroscopic features of **2** vary significantly from those found with complexes of the form  $\text{TpW}(\text{NO})(\text{PMe}_3)(\eta^2\text{-arene})$ . The  $^1\text{H}$  NMR spectrum of **2** features five distinct signals corresponding to phenyl protons ranging from  $\delta$  8.63 to 6.33. No upfield features are present that would be associated with

- \* Corresponding author. E-mail: wdh5z@Virginia.edu.  
 (1) Kiplinger, J. L.; Richmond, T. G.; Osterberg, C. E. *Chem. Rev.* **1994**, *94*, 373.  
 (2) Burdeniuc, J.; Jedlicka, B.; Crabtree, R. H. *Chem. Ber.* **1997**, *130*, 145.  
 (3) Richmond, T. G. In *Topics in Organometallic Chemistry*; Murai, S., Ed.; Springer: New York, 1999; Vol. 3, p 243.  
 (4) Jones, W. D. *J. Chem. Soc., Dalton Trans.* **2003**, 3991.  
 (5) Murphy, E. F.; Murugavel, R.; Roesky, H. W. *Chem. Rev.* **1997**, *97*, 3425.  
 (6) Aizenberg, M.; Milstein, D. *Science* **1994**, *265*, 359.  
 (7) Weydert, M.; Andersen, R. A.; Bergman, R. G. *J. Am. Chem. Soc.* **1993**, *115*, 8837.  
 (8) Edelbach, B. L.; Jones, W. D. *J. Am. Chem. Soc.* **1997**, *119*, 7734.  
 (9) Kiplinger, J. L.; Richmond, T. G. *J. Am. Chem. Soc.* **1996**, *118*, 1805.  
 (10) Kiplinger, J. L.; Richmond, T. G. *J. Chem. Soc., Chem. Commun.* **1996**, 1115.  
 (11) Edelbach, B. L.; Rahman, A. K. F.; Lachicotte, R. J.; Jones, W. D. *Organometallics* **1999**, *18*, 3170.  
 (12) Braun, T.; Perutz, R. N. *Chem. Commun.* **2002**, 2749.  
 (13) Kraft, B. M.; Lachicotte, R. J.; Jones, W. D. *J. Am. Chem. Soc.* **2001**, *123*, 10973.  
 (14) Young, R. J., Jr.; Grushin, V. V. *Organometallics* **1999**, *18*, 294.  
 (15) Whittlesey, M. K.; Perutz, R. N.; Moore, M. H. *Chem. Commun.* **1996**, 787.  
 (16) Aizenberg, M.; Milstein, D. *J. Am. Chem. Soc.* **1995**, *117*, 8674.  
 (17) Jones, W. D.; Partridge, M. G.; Perutz, R. N. *J. Chem. Soc., Chem. Commun.* **1991**, 264.

- (18) Braun, T.; Cronin, L.; Higgitt, C. L.; McGrady, J. E.; Perutz, R. N.; Reinhold, M. *New J. Chem.* **2001**, *25*, 19.  
 (19) Reinhold, M.; McGrady, J. E.; Perutz, R. N. *J. Am. Chem. Soc.* **2004**, *126*, 5268.  
 (20) Clot, E.; Oelckers, B.; Klahn, A. H.; Eisenstein, O.; Perutz, R. N. *Dalton Trans.* **2003**, 4065.  
 (21) Bosque, R.; Clot, E.; Fantacci, S.; Maseras, F.; Eisenstein, O.; Perutz, R. N.; Renkema, K. B.; Caulton, K. G. *J. Am. Chem. Soc.* **1998**, *120*, 12634.  
 (22) Keane, J. M.; Harman, W. D. *Organometallics* **2005**, *24*, 1786.  
 (23) Graham, P.; Meiere, S. H.; Sabat, M.; Harman, W. D. *Organometallics* **2003**, *22*, 4364.

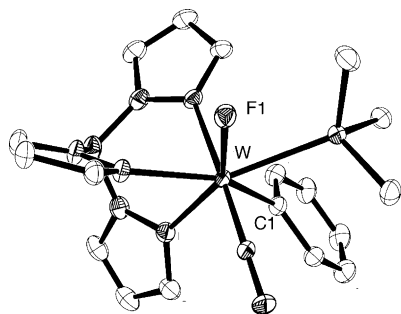


**Figure 1.** ORTEP diagram for the complex  $\text{TpW}(\text{NO})(\text{PMe}_3)(\text{F})(\text{Ph})$  (**2**).  $\text{W}-\text{C}1$ , 2.228(2);  $\text{W}-\text{F}1$ , 2.0052(16) (Å)  $\text{F}1-\text{W}-\text{C}1$  140.34(8) (deg).

an  $\eta^2$ -arene species.<sup>23</sup> The  $^{13}\text{C}$  NMR spectrum shows phenyl carbons in the normal range ( $\delta$  120–130) except for the carbon bound to tungsten ( $\delta$  184), which is coupled by both the fluorine and the phosphine ligands ( $J_{\text{FC}} = 35.8$ ;  $J_{\text{PC}} = 10.7$  Hz). Proton and carbon data clearly indicate that the phenyl ring is unable to undergo rotation about the  $\text{W}-\text{C}$  bond on the time scale of these NMR measurements. NOESY data show an interaction between H6 (6.33 ppm) and  $\text{PMe}_3$  but not for H2 (8.63 ppm). A  $^{31}\text{P}$  NMR spectrum indicates that the fluorine is bound to the metal, exhibiting a doublet ( $J_{\text{F,P}} = 127.0$  Hz) with  $^{183}\text{W}$  satellites ( $J_{\text{W,P}} = 212.5$  Hz). The  $^{19}\text{F}$  NMR spectrum also shows this coupling ( $J_{\text{F,P}} = 127.0$  Hz), but here  $^{183}\text{W}$  satellites were not observed, even though  $^{183}\text{W}-^{19}\text{F}$  coupling has been detected in a few higher oxidation state complexes.<sup>24–26</sup> IR data show an absorption associated with an NO stretch at  $1596\text{ cm}^{-1}$ , a feature significantly blue-shifted from common  $\eta^2$ -coordinated arene- $\text{W}^0$  complexes (e.g., **1**:  $\nu_{\text{NO}} = 1564\text{ cm}^{-1}$ ).<sup>27</sup> Cyclic voltammetric data for **2** show only a broad oxidation wave with  $E_{\text{p,a}}$  near 1.5 V (NHE), well beyond the normal range of  $\text{TpW}^0(\text{NO})(\text{PMe}_3)$  complexes.<sup>22</sup> Ultimately, crystals were grown from a  $\text{CDCl}_3$  and pentane solution and X-ray structure determination was carried out. An ORTEP diagram of **2** appears in Figure 1.

The formation of the phenyl fluoride complex **2** occurs under exceptionally mild conditions, compared with other examples of  $\text{C}-\text{F}$  activation with fluorobenzene in the literature.<sup>13,14</sup> The reaction was monitored by  $^{31}\text{P}$  NMR and the results show that the reaction reaches 50% completion in 3.3 h at 22 °C, a half-life similar to other reactions of **1** in which the rate is determined by benzene dissociation (e.g., formation of **3**; *vide infra*).

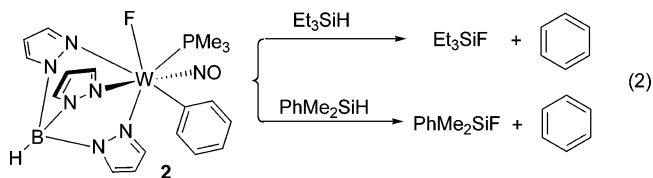
During the course of the reaction in neat fluorobenzene, a small amount of a transient species was detected in the  $^{31}\text{P}$  NMR spectrum with a  $^{31}\text{P}\{^1\text{H}\}$  signal at  $\delta -8.49$  ( $J_{\text{W,P}} = 239$  Hz), which did not show coupling to fluorine, that vanished as the reaction approached completion. A corresponding signal was not detected in the  $^{19}\text{F}$  NMR spectrum. Judging from the chemical shift and  $J_{\text{W,P}}$  coupling constant in the phosphorus data, we can rule out a purported aryl hydride or aryl fluoride intermediate, and we speculate that the transient species may be an  $\eta^2\text{-C}_6\text{H}_5\text{F}$  complex analogous to **1**.

Complex **2** is remarkably stable both as a solid and in solution, even at elevated temperatures. In a DMF solution at 100 °C for 0.5 h, less than 5% decomposition is observed. However, when a solution of **2** is subjected to triethylsilane

**Table 1.**

Ligand	Product	

( $\text{Et}_3\text{SiH}$ ) in  $\text{CDCl}_3$ , fluorotriethylsilane and free benzene are readily formed (eq 2). Supporting evidence for the formation of  $\text{FSiEt}_3$  includes a  $^{19}\text{F}$  NMR resonance at  $-176.4$  ppm (sep,  $J = 6.1$  Hz) and a GC-MS trace with  $m/z = 134$  ( $\text{M}^+$ ). The amount of free benzene produced was determined to be about 70% based on  $^1\text{H}$  NMR integration, relative to a durene standard. The metal fragment decomposes to give only paramagnetic materials. Attempts to trap the metal fragment with a variety of potential ligands (acetone, cyclopentene, fluorobenzene) failed to give an identifiable tungsten complex. Similarly, the reaction of  $\text{PhMe}_2\text{SiH}$  and **2** in  $\text{CDCl}_3$  gave  $\text{PhMe}_2\text{SiF}$ , as identified by  $^{19}\text{F}$  NMR ( $-162.1$  ppm) and GC-MS ( $m/z$  154 ( $\text{M}^+$ )).



**$\eta^2$ -Coordination versus  $\text{C}-\text{F}$  Activation.** The reactions of **1** with several other fluorinated arenes were studied, and the results are summarized in Table 1. When the benzene complex **1** was treated with  $\alpha,\alpha,\alpha$ -trifluorotoluene, two coordination diastereomers, **3A** and **3B** (1.2:1), were obtained with a half-life of approximately 3 h (22 °C). Both **3A** and **3B** are readily

(24) Postel, U.; Riess, J. G.; Claves, J. Y.; Guerschais, J. *Inorg. Chim. Acta* **1979**, *32*, 175.

(25) Wray, V. *Annu. Rep. NMR Spectrosc.* **1983**, *14*, 365.

(26) Quinones, G. S.; Hagele, G.; Seppelt, K. *Chem.-Eur. J.* **2004**, *10*, 4755.

(27) Graham, P. M.; Meiere, S. H.; Sabat, M.; Harman, W. D. *Organometallics* **2003**, *22*, 4364.

identifiable as  $\eta^2$ -coordinated arene complexes. The  $^1\text{H}$  NMR spectrum of **3** shows diagnostic resonances at 3.95 (**3A**), 3.77 (**3B**), 2.43 (**3A**), and 2.30 (**3B**) ppm, corresponding to protons associated with the bound carbons. An NO stretch at  $\nu_{\text{NO}} = 1575 \text{ cm}^{-1}$  (cf.  $\nu_{\text{NO}} = 1564 \text{ cm}^{-1}$  for **1**) and an oxidation wave with  $E_{\text{p,a}} = 0.06 \text{ V}$  (NHE; cf.  $-0.13 \text{ V}$  at 100 mV/s for **1**) indicate that trifluorotoluene is a better  $\pi$ -acid and/or worse  $\sigma$ -donor than benzene. As a result, complexes **3A** and **3B** are more stable than their benzene analogue, both thermally and chemically. For example, a ligand exchange reaction of  $\text{CF}_3\text{Ph}$  for acetone (**3** dissolved in acetone- $d_6$ ) is ca. 250 times slower than that for the benzene analogue. While no C–F activated product was observed, a trace amount (5%) of what is thought to be the C–H insertion product  $\text{TpW}(\text{NO})(\text{PMe}_3)(\text{CF}_3\text{C}_6\text{H}_4)\text{-(H)}$  is detectable in the  $^1\text{H}$  and  $^{31}\text{P}$  NMR spectra (*vide infra*). The key features supporting this assignment are two W–H signals at  $\delta$  9.32 and 9.35 ppm, each strongly coupled by  $^{31}\text{P}$  ( $\sim 102 \text{ Hz}$ ). These features are similar to several other tungsten hydride species recently observed in our laboratories.<sup>28</sup> There was not a sufficient amount formed for either species to determine which C–H bond (if two atropisomers) or bonds (if constitutional isomers) were activated. Finally, a competitive rate experiment was performed in which the benzene complex **1** was dissolved in a 1:1 mixture of fluorobenzene and  $\alpha,\alpha,\alpha$ -trifluorotoluene, and the reaction was monitored by  $^{31}\text{P}$  NMR.<sup>29</sup> Over the course of this reaction, the two products, **2** and **3**, formed in a 1:1 ratio. These observations are consistent with a common, rate-limiting step for these two reactions in which benzene dissociates from **1**, followed by the coordination of either trifluorotoluene or fluorobenzene by  $\{\text{TpW}(\text{NO})(\text{PMe}_3)\}$  with similar activation energies.

In contrast to what is observed with  $\alpha,\alpha,\alpha$ -trifluorotoluene, the reaction of **1** with 1-fluoro-3-(trifluoromethyl)benzene exclusively produced the C–F activated product, as a mixture of two atropisomers (**4A** and **4B**, 5:4 ratio). Complexes **4A** and **4B** show similar spectroscopic features to **2**, each with four well-defined phenyl hydrogens and six ring carbons. While we cannot rule out that **4A** and **4B** are coordination diastereomers (e.g., where the aryl and fluoride ligands are transposed), the high barrier to ring rotation seen in **2** will certainly be present in **4** as well, and the remote location of the  $\text{CF}_3$  group makes it unlikely that one atropisomer would be strongly favored kinetically or thermodynamically over the other.<sup>30</sup> Although we expect that 1-fluoro-3-(trifluoromethyl)benzene is a better  $\pi$ -acid than trifluoromethylbenzene and, thus, would form more stable  $\eta^2$ -arene complexes with  $\{\text{TpW}(\text{NO})(\text{PMe}_3)\}$ , none was observed, nor was there any sign of a purported C–H addition product.

Considering the above results with fluorobenzene and 1-fluoro-3-(trifluoromethyl)benzene, aromatic carbon–fluorine bonds should be kinetically accessible to the  $\{\text{TpW}(\text{NO})(\text{PMe}_3)\}$  fragment. However, the reaction of **1** with hexafluorobenzene generates an  $\eta^2$ -coordinated arene product (**5**), with no C–F activation products being observed. While only limited information is provided by the  $^1\text{H}$  NMR spectrum due to the absence of phenyl protons,  $^{31}\text{P}$  NMR ( $\delta$   $-111.1$ ,  $J_{\text{F,P}} = 4.1 \text{ Hz}$ ) and  $^{19}\text{F}$  NMR (six signals ranging from  $\delta$   $-144.8$  to  $-187.3$ , one weakly split by  $^{31}\text{P}$  ( $4.1 \text{ Hz}$ )) indicate that **5** is an  $\eta^2$ -coordinated  $\text{W}^0$  complex rather than a  $\text{W}^{\text{II}}$  metal fluoride. Cyclic voltammetric

data show an oxidation wave ( $E_{\text{p,a}} = -0.19 \text{ V}$ ) very close to that of the benzene analogue **1**.<sup>31</sup> However, infrared data for **5** ( $\nu_{\text{NO}} = 1616 \text{ cm}^{-1}$ ) more closely resemble that of the aryl fluorides **2** and **4** (cf. the  $\eta^2$ -arene complexes **1** and **3**). This discrepancy is likely due to the highly electron-deficient nature of  $\text{C}_6\text{F}_6$ . Nucleophilic aromatic substitution reaction mechanisms ( $\text{S}_{\text{N}}\text{Ar}$ ) are commonly invoked for C–F bond activation. Were this mechanism operative for  $\{\text{TpW}(\text{NO})(\text{PMe}_3)\}$ , increasing the fluorination on the aromatic ring would be expected to enhance the rate of the C–F activation reaction. Furthermore, calculations by others suggest that the M–Ar bond becomes stronger as the fluorine content of the aryl ring (Ar) increases. Even though the  $\text{C}_6\text{H}_5\text{–F}$  bond is ca. 30 kcal/mol weaker than the  $\text{C}_6\text{F}_5\text{–F}$  bond,<sup>32</sup> hexafluorobenzene generally undergoes C–F activation much more readily than fluorobenzene. The opposite is observed for the reaction of these fluorobenzenes with  $\{\text{TpW}(\text{NO})(\text{PMe}_3)\}$ . Hexafluorobenzene is expected to be a better  $\pi$ -acid than benzene, and apparently this factor along with the stronger C–F bond energy<sup>32</sup> make the  $\eta^2$ -arene complex more favorable than the corresponding C–F adduct. Within hours solutions of this complex decompose to uncharacterized paramagnetic products.

Dihapto-coordinated arene complexes were also observed when 1-fluoronaphthalene was combined with the benzene complex. In this case the reaction afforded four constitutional isomers, **6A–6D**, all of which were determined to be  $\eta^2$ -coordinated arenes. No C–F activated products nor C–H activated species were detected (upper limit: 2%). We attribute this contrasting result to the well-documented increase in stability observed for  $\eta^2$ -naphthalene complexes compared to their  $\eta^2$ -benzene analogues.<sup>33–35</sup> NMR (bound protons: 3.81, 3.60, 2.64, 2.35, 2.25 ppm; bound carbons:  $\delta$  59.6, 58.5, 58.4, 58.3, 58.3, 58.1, 55.1, 55.3), IR ( $\nu_{\text{NO}} = 1573 \text{ cm}^{-1}$ ), and CV ( $E_{\text{p,a}} = 0.17 \text{ V}$ ) data strongly support the assignment of  $\eta^2$ -coordinated complexes and closely resemble these data for previously reported  $\eta^2$ -naphthalene complexes of rhenium<sup>36</sup> and molybdenum.<sup>37</sup> Upon heating a solution of this mixture to 100 °C in DMF- $d_7$  for 30 min, **6A** and **6B** were completely absent, while isomers **6C** and **6D** suffered a 65% loss in intensity, and free 1-fluoronaphthalene appeared. Yet, no oxidative addition product was detected. These observations suggest that **6A** and **6B** were not in equilibrium with **6C** and **6D** in the initial observed ratio of 1:1:1:1. Rather, these data reflect the nearly identical rates of tungsten coordination for the two rings (fluorinated and unfluorinated).<sup>38</sup> When a solution of **6** is treated with triethylsilane, no fluorotriethylsilane was formed after 24 h.

**C–H Activation.** During the course of these studies, minor amounts of two hydridic intermediates were detected in solution

(31) It is possible that in this case  $E_{\text{p,a}}$  is not a good reflection of the formal reduction potential,  $E^\circ$ , because of an exceptionally fast chemical reaction (substitution) following the electrochemical event (EC) mechanism. This would shift the anodic peak negative.

(32) Smart, B. E. In *The Chemistry of Functional Groups, Supplement*; Patai, D. S., Rappoport, Z., Eds.; Wiley: New York, 1983; Chapter 14.

(33) Ha, Y.; Dilsky, S.; Graham, P. M.; Liu, W.; Reichart, T. M.; Sabat, M.; Keane, J. M.; Harman, W. D. *Organometallics* **2006**, *25*, 5184.

(34) Winemiller, M. D.; Kelsch, B. A.; Sabat, M.; Harman, W. D. *Organometallics* **1997**, *16*, 3672.

(35) Chin, R. M.; Dong, L.; Duckett, S. B.; Jones, W. D. *Organometallics* **1992**, *11*, 871.

(36) Meiere, S. H.; Brooks, B. C.; Gunnoe, T. B.; Carrig, E. H.; Sabat, M.; Harman, W. D. *Organometallics* **2001**, *20*, 3661.

(37) Meiere, S. H.; Keane, J. M.; Gunnoe, T. B.; Sabat, M.; Harman, W. D. *J. Am. Chem. Soc.* **2003**, *125*, 2024.

(38) **6A** and **6B** are almost certainly in equilibrium, based on our previous examination of intraannular and interannular isomerization rates for naphthalenes.

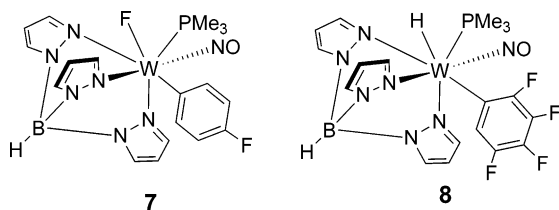
(28) Graham, P. M.; Delafuente, D. A.; Liu, W.; Myers, W. H.; Sabat, M.; Harman, W. D. *J. Am. Chem. Soc.* **2005**, *127*, 10568.

(29) Integration ratios in a  $^{31}\text{P}$  NMR spectrum closely matched that observed in a  $^1\text{H}$  NMR spectrum for an authentic mixture of **2** and **3**.

(30) By this reasoning, two atropisomers are expected and only two isomers are experimentally observed.

of the trifluorotoluene complex **3** (*vide supra*). Suspecting that these may be aryl hydride species, we carefully examined solutions of the benzene precursor **1** for the analogous hydride. While no hydridic signal could be detected in  $CDCl_3$ , in acetone- $d_6$  a doublet with  $J_{P,H} = 101$  Hz appeared far *downfield* at  $\delta$  9.32,<sup>39</sup> integrating to approximately 20% of one proton for the benzene complex. As time passed, the benzene complex slowly gave way to formation of the acetone complex,  $TpW(NO)(PMe_3)(\eta^2\text{-acetone})$  (**6**).<sup>40</sup> During the course of this reaction the ratio of the presumed hydride  $TpW(NO)(PMe_3)(Ph)(H)$  (**1H**) and benzene (**1**) complexes was monitored by  $^1H$  NMR and remained constant at 1:4 until both signals vanished. Accompanying the hydride signal was a  $PMe_3$  signal at  $\delta$  1.50 and a collection of  $Tp$  resonances and phenyl peaks, some overlapping the benzene complex, which also faded over time. Similar results were obtained in the  $^{31}P$  NMR spectra, where a signal at  $\delta = -3.15$  ppm ( $d$ ,  $J_{WP} = 174$  Hz) corresponding to the hydride complex remained at 20% of the signal for **1** throughout the substitution reaction. Although solution IR data (DME) failed to show an additional nitrosyl or hydride peak, NMR data indicate that an equilibrium exists between  $TpW(NO)(PMe_3)(\eta^2\text{-benzene})$  and  $TpW(NO)(PMe_3)(Ph)(H)$ , as well as between the trifluorotoluene and trifluorotoluylyl hydride analogues, and suggests that *if* a transient  $\eta^2\text{-fluorobenzene}$  complex is formed in the formation of **2**, the aryl hydride species is also likely to be kinetically accessible.

In addition to the preparative reactions described above, the reactions of the benzene complex **1** with two other fluorobenzenes were briefly explored using  $^{31}P$  NMR. When **1** was dissolved in a DME solution of 1,4-difluorobenzene, a new resonance grew in at  $\delta$  8.19 (80%), showing a PF coupling constant of 128.9 Hz.<sup>41</sup> Given the similarity of these values to **2** and **4**, C–F activation to form **7** is indicated. Repeating this experiment with 1,2,3,4-tetrafluorobenzene gave a complicated  $^{31}P$  NMR spectrum, but the major product (50%) features a resonance with chemical shift  $\delta$  (–1.06) and tungsten–phosphorus coupling (169 Hz) consistent with an *aryl hydride* complex. An  $^1H$ NMR spectrum of the recovered reaction mixture shows a hydride signal at  $\delta$  9.05 ( $d$ ,  $J_{PH} = 109$  Hz), supporting the hypothesis of a C–H addition reaction leading to the formation of **8**.



**Mechanism of C–F Activation.** Two landmark DFT studies have been carried out exploring the competing reaction pathways for C–H and C–F oxidative addition for arenes. In 1998, Caulton, Eisenstein, and Perutz<sup>14</sup> examined these reactions for  $CpRh(PH_3)$  and  $Os(H)(CO)(PH_3)_2$ , and in 2004 McGrady and Perutz<sup>24</sup> investigated the  $Ni(H_2PCH_2CH_2PH_2)$  and  $Pt(H_2PCH_2CH_2PH_2)$  systems. In both studies, an  $\eta^2\text{-arene}$  complex was thought to be an intermediate on the reaction coordinate for either C–H or C–F activation. While this is a possibility in

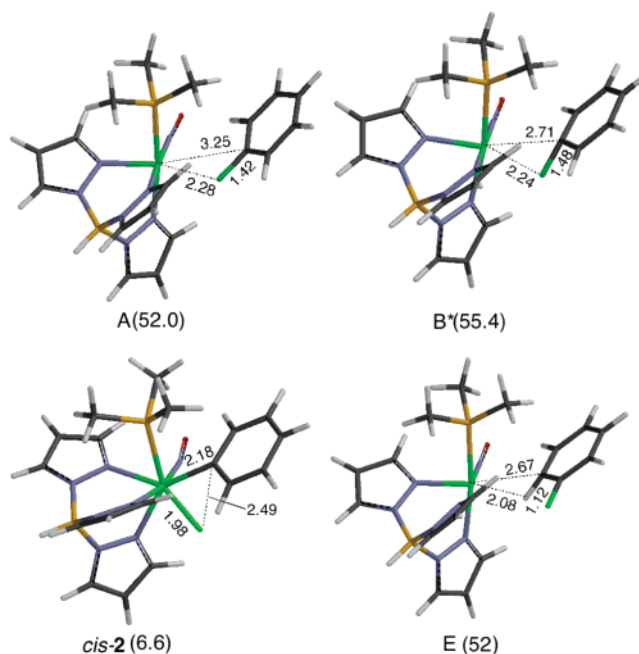


**Figure 2.** Optimized geometry for the  $\kappa F$  complex (**A**) the transition state (**B\***) and the C–F insertion product *cis*-**2** leading to the formation of *trans*-**2**, and the purported  $\kappa H$  complex (**E**) (relative energy, kcal/mol).

the present tungsten system as well, we also considered the possibility that the  $\eta^2\text{-species}$  was a mechanistic dead-end and that the C–F activation could take place directly from a  $\sigma$ -complex in which either the fluorine atom or C–F bond was coordinated. To investigate this, we carried out DFT calculations using the Gaussian 03 program suite.<sup>42</sup> Relative energies were determined using the LSDA density functional. The model incorporates the Los Alamos pseudopotential LANL2DZ and the associated basis functions.<sup>43–45</sup> This combination has proved informative for Os, Mo, Re, and W systems in determining accurate geometries;<sup>46</sup> however, it tends to overestimate bond energies. Given the dissociative nature of substitution reactions with the benzene complex **1** (*vide supra*), we did not explore an alternative reaction mechanism in which the nitrosyl bends to create an open coordination position for the fluorobenzene. These calculations reveal a direct route to C–F activation that passes through a *fluorine-bound* intermediate (**A**) stabilized by 20 kcal compared with the dissociated species (Figure 2). Interestingly, the fluorobenzene approaches the  $\{TpW(NO)(PMe_3)\}$  fragment with the aryl group oriented toward the  $PMe_3$  group. The W–F–C bond angle in **A** is  $121^\circ$ , allowing the metal to partially overlap with the C–F  $\sigma^*$  orbital, and in response, the C–F bond is lengthened from 1.38 to 1.42 Å. As the phenyl draws closer to the metal, the C–F bond continues to stretch to 1.48 Å, the W–F–C bond angle closes to  $90^\circ$ , and a modest 3 kcal/mol barrier is reached in the transition state (**B\***; Figures 2 and 3). The formation of *cis*-**2** lies just beyond this transition state, but apparently the steric interaction between the  $PMe_3$  and the adjacent rigid pyrazole ring causes *cis*-**2** to be unstable with respect to its isomer *trans*-**2**. For this experimentally observed form, the ipso carbon and the fluorine still lie in a plane perpendicular to the M–N–O bond axis, but are no longer

(39) Graham, P. M.; Mocella, C. J.; Sabat, M.; Harman, W. D. *Organometallics* **2005**, *24*.

(40) Originally this is formed as the kinetic isomer in which O is oriented away from the phosphine. Over time this rearranges to the thermodynamic isomer in which the oxygen is oriented toward the phosphine.

(41) A second, small coupling constant is also present of  $J = 5.9$  Hz.

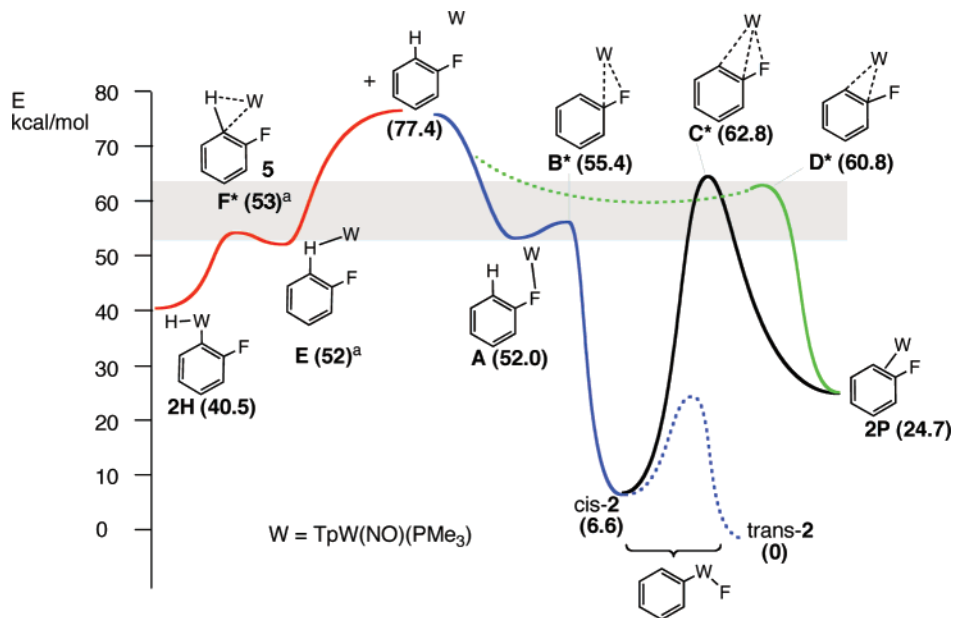
(42) Frisch, M. J., et al. *Gaussian 03*, Revision C.02; Gaussian, Inc.: Wallingford, CT, 2004.

(43) Hay, P. J.; Wadt, W. R. *J. Chem. Phys.* **1985**, *82*, 270.

(44) Wadt, W. R.; Hay, P. J. *J. Chem. Phys.* **1985**, *82*, 284.

(45) Hay, P. J.; Wadt, W. R. *J. Chem. Phys.* **1985**, *82*, 299.

(46) Trindle, C. O.; Harman, W. D. *J. Comput. Chem.* **2005**, *26*, 194.



a. see reference 49

**Figure 3.** Reaction coordinate diagram for C–F and C–H activation of fluorobenzene by  $\{\text{TpW}(\text{NO})(\text{PMe}_3)\}$ .

adjacent (see Figure 1), and the  $\text{PMe}_3$  is no longer in the proximity of the heterocycle rings. We note that by this route  $\eta^2$ -coordination does not lie on the reaction pathway and is, in fact, counterproductive. Such a path is reminiscent of the classic study by Bergman and Stoutland, who first demonstrated that a transition metal ( $\text{Cp}^*\text{Ir}(\text{PMe}_3)$ ) could insert into the C–H bond of ethene without first binding it  $\eta^2$ .<sup>47</sup> A similar conclusion was recently reached for the tungsten insertion into a benzene C–H bond.<sup>48</sup>

A striking feature of the  $\eta^1$ -reaction pathway is the low activation barrier for C–F activation (the rate of formation of **2** is determined by benzene dissociation from **1**). The calculated difference of only 0.1 Å between free ligand and the transition state of **2** is in stark contrast to the 0.28 Å lengthening reported for  $[\text{CpRh}(\text{PH}_3) + \text{C}_6\text{H}_4\text{F}_2]$ <sup>21</sup> or the 0.21 Å distortion calculated for  $[\text{Pt}(\text{H}_2\text{PCH}_2\text{CH}_2\text{PH}_2) + \text{C}_6\text{F}_6]$ .<sup>19</sup> The markedly earlier transition state calculated for the formation of **2**, which leads to its facile formation, is likely a direct result of the highly electron-rich nature of the  $\{\text{TpW}(\text{NO})(\text{PMe}_3)\}$  fragment. Similar to the present case is the system  $[\text{Ni}(\text{H}_2\text{PCH}_2\text{CH}_2\text{PH}_2) + \text{C}_6\text{F}_6]$ ,<sup>19</sup> which shows a distortion of only 0.13 Å between free ligand and transition state. For this  $\text{Ni}^0$  system, the activation barrier is low enough that C–F activation dominates over C–H activation.

For the purpose of comparison, we have also calculated the energy of a purported  $\eta^2$ -fluorobenzene intermediate (**2P**) in which C1 and C2 are coordinated (Figure 3). While this 1,2- $\eta^2$ -isomer is likely not the most stable  $\eta^2$ -form due to the disruption of C–F conjugation,<sup>20</sup> it is the intermediate most competent to undergo direct C–F activation. The  $\eta^2$ -arene species (**2P**) was located 24.7 kcal/mol higher than the experimentally observed C–F activation product *trans*-**2**, which in turn is found to be 6 kcal/mol lower in energy than isomer *cis*-**2**. A transition state (**C\***) was ultimately located between the  $\eta^2$ -arene species and the purported species *cis*-**2**, about 38 kcal/mol above the  $\pi$ -complex **2P**. In addition, a second

activation barrier (**D\***) was located leading to the  $\eta^2$ -complex, which does not involve a significant W–F interaction. This transition state may be along a separate energy pathway leading from fragments directly to  $\eta^2$ -coordination, but no other intermediates could be identified. Given that substitution of the benzene ligand in **1** is largely dissociative,<sup>49,50</sup> and the observation that **2** and **3** are formed in a 1:1 ratio from a 1:1 solution of fluorobenzene and trifluorotoluene, the formation of the  $\eta^2$ -species **2P** is probably kinetically competitive with C–F activation, but the former (**2P**) is thermodynamically inferior.

**Mechanism of C–H Activation.** The  $d^6$  system  $\text{CpRe}(\text{CO})_2$  is isoelectronic to  $\{\text{TpW}(\text{NO})(\text{PMe}_3)\}$  and has been extensively studied with fluoroarenes in the context of C–H activation.<sup>20</sup> As with other systems described, when this metal reacts with fluorobenzenes containing aryl hydrogens, C–H activation is observed exclusively.<sup>51</sup> Why then is C–F activation not preempted by C–H activation for the tungsten system? To address this question, we next explored the reaction pathway for the insertion of  $\{\text{TpW}(\text{NO})(\text{PMe}_3)\}$  into the C–H bond of fluorobenzene. Similar to that found with C–F activation, DFT calculations identified a  $\kappa\text{H}$  complex, **E** (Figure 2), stabilized by about 25 kcal/mol compared to the reaction fragments. This agostic interaction is characterized by a slightly elongated C–H bond (1.12 Å), a W–H bond length of about 2.1 Å, and a W–H–C bond angle of 130°. As with the  $\kappa\text{F}$  intermediate, the phenyl is oriented toward the  $\text{PMe}_3$  group. From this point, passage through a nearby but not fully defined transition state **F\***<sup>52</sup> leads to the formation of the C–H insertion product **2H** (Figure 3), found to be about 40 kcal/mol above the experimentally observed C–F isomer *trans*-**2**. Others have suggested that an  $\eta^2$ -arene complex is not a required precursor to C–H activation,<sup>48,53–55</sup> and Parkin et al.<sup>48</sup> have reported computational evidence for a  $\kappa\text{H}$  intermediate leading to Ph–H insertion by tungsten.

While the insertion of tungsten into the C–H bond is apparently facile, it is not thermodynamically viable, at least

(47) Stoutland, P. O.; Bergman, R. G. *J. Am. Chem. Soc.* **1985**, *107*, 4581.

(48) Churchill, D. G.; Janak, K. E.; Wittenberg, J. S.; Parkin, G. *J. Am. Chem. Soc.* **2003**, *125*, 1403.

(49) The half-life for benzene substitution at 22 °C is largely unaffected by either the nature or the concentration of the incoming ligand.

(50) Bengali, A.; Leicht, A. *Organometallics* **2001**, *20*, 1345.

(51) Godoy, F.; Higgitt, C. L.; Klahn, A. H.; Oelckers, B.; Parsons, S.; Perutz, R. N. *Dalton Trans.* **1999**, 2039.

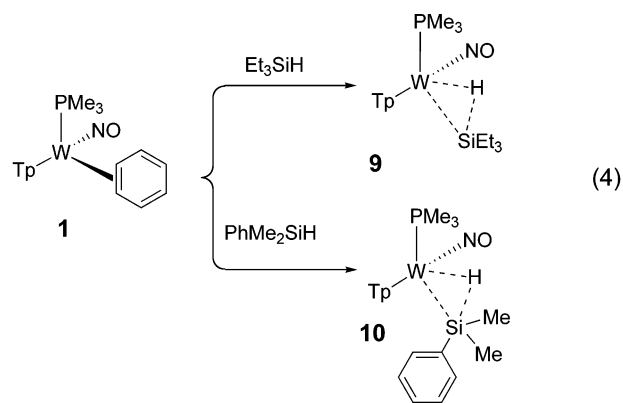
for fluorobenzene. We note that the calculated energy of the purported C–H insertion product for fluorobenzene (**2H**) is not far from that of the purported  $\eta^2$ -arene **2P**, in line with what we observe for **1**. A summary of the reaction coordinate diagram for C–H and C–F addition is shown in Figure 3. Collectively these DFT calculations describe a number of weakly associated intermediates with low-energy associated activation barriers, all located about 20 kcal/mol below the reaction fragments (gray zone in Figure 3). From here, C–H insertion, C–F insertion, and  $\eta^2$ -formation pathways diverge with neither insertion mechanism apparently requiring  $\eta^2$ -coordination as a preceding event.

Our observations with 1,2,3,4-tetrafluorobenzene suggest that as more fluorines are added and the benzene ring loses electron density, C–H activation becomes competitive with both C–F activation and  $\eta^2$ -coordination. The latter point was made previously by Clot and Perutz in a DFT study of C–H oxidative addition with the complex {CpRe(CO)<sub>2</sub>} and various partially fluorinated benzenes.<sup>20</sup> These authors concluded that as the number of fluorine atoms in the ring increased, the M–aryl bond strength increased, thus increasing the likelihood of oxidative addition. As we observed for benzene, C–H activation is likely to be reversible for mono- and difluorinated benzenes with the {TpW(NO)(PMe<sub>3</sub>)} system, and C–F activation ultimately dominates. For tetrafluorobenzene and hexafluorobenzene, however, C–F activation no longer is observed. Whether this is a reflection of an increased activation barrier to C–F activation for these systems or a shift in the relative stabilities of the different isomers remains unclear for the tungsten system.

**$\eta^2$ -Silane Complexes.** As part of this study, silanes were used to convert aryl fluorides into free arenes (*vide supra*). Therefore, we spectroscopically investigated the reaction of the benzene complex **1** with triethylsilane and phenyldimethylsilane as a control. When **1** was treated with triethylsilane, a new complex (**9**) was obtained that has an empirical formula consistent with TpW(NO)(PMe<sub>3</sub>)·Et<sub>3</sub>SiH according to its spectroscopic features. A <sup>1</sup>H NMR spectrum shows a Si–H–W resonance at  $\delta$  3.85 that is coupled to the PMe<sub>3</sub> ( $J_{\text{PH}} = 64.2$  Hz) and shows slightly

larger coupling to <sup>183</sup>W ( $J_{\text{W,H}} = 39.6$  Hz) than other complexes of the form TpW(NO)(PMe<sub>3</sub>)(H)(L) (15–33 Hz). Significantly, <sup>29</sup>Si coupling (4.7% abundance) to this proton was *not* observed. While it is possible that a coincidental overlap with the <sup>183</sup>W satellites obscured these low-intensity signals, we can confidently state that <sup>1</sup>J<sub>Si,H</sub> is no greater than about 40 Hz. These observations along with the absence of any significant three-bond coupling (<sup>3</sup>J<sub>H<sub>Si</sub>CH</sub> < 3 Hz) indicates a major disruption of the Si–H bond. However, both the chemical shift for the hydride ( $\delta$  3.85) and the associated coupling constant  $J_{\text{P,H}}$  (64.2 Hz) are well below those values of classical TpW(NO)(PMe<sub>3</sub>)(H)(L) complexes (typically  $\delta$  9–13 with  $J \approx 100$  Hz).<sup>39</sup> Further, the <sup>31</sup>P chemical shift of  $\delta$  –11.36 and associated  $J_{\text{WP}} = 242.9$  Hz fall well outside the normal range of W(II) hydride complexes for this system ( $\delta$  +10 to –5; 100–130 Hz).<sup>28</sup> IR data for **9** show an  $\nu_{\text{NO}}$  at 1566 cm<sup>–1</sup>, and a cyclic voltammogram of this material features an anodic wave at  $E_{\text{p,a}} = +0.34$  V (100 mV/s). These infrared and electrochemical features are similar to  $\eta^2$ -alkene and  $\eta^2$ -arene complexes of {TpW(NO)(PMe<sub>3</sub>)}, but are fully inconsistent with the known examples of the seven-coordinate W(II) complexes of the type TpW(NO)(PMe<sub>3</sub>)(H)(L) and TpW(NO)(PMe<sub>3</sub>)(F)(Ar).<sup>28</sup> The reaction of dimethylphenylsilane with **1** provides similar results, forming a complex (**10**) with spectroscopic features closely resembling those of **9**. When either **9** or **10** is dissolved in acetone-*d*<sub>6</sub> and heated to 55 °C for several hours, no ligand exchange was observed. However, attempts to recrystallize these materials for X-ray or combustion analysis resulted in their decomposition.

Silane  $\sigma$ -complexes with transition metals are well documented.<sup>56–63</sup> Most relevant to the present study are reports from Schubert et al. regarding related W(CO)<sub>5</sub> and W(CO)<sub>4</sub>(PR<sub>3</sub>) analogues to **9** and **10**.<sup>64</sup> While strong <sup>183</sup>W–H coupling and the absence of a large <sup>1</sup>J<sub>SiH</sub> and <sup>3</sup>J<sub>H<sub>Si</sub>CH</sub> coupling in **9** or **10** clearly indicate the degradation of the Si–H bonds,<sup>64</sup> the infrared and electrochemical data suggest that these complexes should probably be regarded as “stretched”  $\sigma$ -complexes rather than classical silyl hydrides (eq 4).



### Concluding Remarks.

Mono- and difluorinated benzenes undergo facile oxidative addition with the {TpW(NO)(PMe<sub>3</sub>)} system, forming seven-coordinate aryl fluoride complexes. DFT calculations reveal two viable reaction pathways, one passing through an  $\eta^2$ -arene

(52) The approach of fluorobenzene to the agent [W] was traced for two pathways, with the reaction coordinate being the W–F or W–H distance, respectively. The first pathway led to a well-defined equilibrium complex **A** and a transition state **B**\* from which the CF activated product derives. The second pathway led smoothly to the CH activation product. Since pure density functionals are known to underestimate activation barriers (see Stanton, R. V.; Merz, Jr, K. M. *J. Chem. Phys.* **1994**, *100*, 434) and LSDA in particular overestimates binding energy in stable molecules, and because an admixture of HF exchange into the density functional, such as is done in the B3LYP formulation, improves estimates of barrier heights relative to those obtained by pure DFT functionals, we retraced the path with B3LYP/LANL2DZ model chemistry calculations. This produced a shallow minimum with an activation barrier no greater than 1 kcal/mol. We reoptimized the structure of the weak complex, constraining the C–H and H–W distances and the C–H–W angle to the values obtained in B3LYP/LANL2DZ. The energies quoted in the text for the CH complex and the transition state on the path toward the CH activated structure are LSDA/LANL2DZ values obtained at these constrained structures. We are confident in the values of the energies of these points along the CH activation path within 5 kcal/mol or less and consider that the values quoted are upper bounds to the values at corresponding points on the fully optimized path. For more on the use of LSDA in organometallic structures see: Salahub, D. R.; Chretien, S.; Milet, A.; Proynov E. I. In *ACS Symp. Ser. 721*; ACS: Washington, DC, 1999. Koch, W.; Holthausen, M. C. In *A Chemist's Guide to Density Functional Theory*, 2nd ed.; Truhlar, D. G., Morokuma K., Eds.; Wiley-VCH: Weinheim, Germany 2001.

(53) Vignalok, A.; Uzan, O.; Shimon, L. J. W.; Ben-David, Y.; Martin, J. M. L.; Milstein, D. *J. Am. Chem. Soc.* **1998**, *120*, 12539.

(54) Johansson, L.; Tilset, M.; Labinger, J. A.; Bercaw, J. E. *J. Am. Chem. Soc.* **2000**, *122*, 10846.

(55) Wik, B. J.; Lersch, M.; Krivokapic, A.; Tilset, M. *J. Am. Chem. Soc.* **2006**, *128*, 2682.

(56) Hart-Davis, A. J.; Graham, W. A. *G. J. Am. Chem. Soc.* **1971**, *93*, 4388.

(57) Corey, J. Y.; Braddock-Wilking, J. *Chem. Rev.* **1999**, *99*, 175.

(58) Schubert, U. In *Advances in Organosilicon Chemistry*; Marciniac, B., Chojnowski, J., Eds.; Gordon and Breach: Yverdon-les-Bains, Switzerland, 1994.

(59) Schubert, U. In *Progress in Organosilicon Chemistry*; Marciniac, B., Chojnowski, J., Eds.; Gordon and Breach: Switzerland, 1995; p 287.

intermediate and one passing through a  $\kappa$ F complex (**A**). From complex **A**, a modest 3 kcal/mol barrier is estimated to stand in the way of C–F activation, offering an explanation for the uncommonly rapid insertion of the metal. In contrast to reports of other second- or third-row transition metal complexes, C–H addition is not observed with mono- or difluorinated benzenes, though this reaction is thought to be kinetically accessible. When the number of fluorines increases to four, C–H insertion becomes competitive, and for hexafluorobenzene or fluoronaphthalene,  $\eta^2$ -coordination dominates.

### Experimental Section.

**General Methods.** NMR spectra were obtained on a 300 or 500 MHz Varian INOVA spectrometer. All chemical shifts are reported in ppm and are referenced to tetramethylsilane (TMS) utilizing residual  $^1\text{H}$  or  $^{13}\text{C}$  signals of the deuterated solvents as an internal standard.  $^{19}\text{F}$  NMR spectra were referenced to trichlorofluoromethane ( $\text{CFCl}_3$ ,  $\delta = 0.00$  ppm with downfield chemical shifts taken to be positive) using trifluoromethylbenzene ( $\delta = -63.72$  ppm) as an internal standard.  $^{31}\text{P}$  NMR spectra were referenced to 85%  $\text{H}_3\text{PO}_4$  ( $\delta = 0.00$  ppm) using triphenyl phosphate ( $\delta = -16.58$  ppm) as an internal standard. Coupling constants ( $J$ ) are reported in hertz (Hz). Resonances in the  $^1\text{H}$  NMR spectrum due to pyrazole ligands (Tp) are listed by chemical shift and multiplicity only (all coupling constants are 2 Hz). Infrared spectra (IR) were recorded on a MIDAC Prospect Series (Model PRS) spectrometer as a glaze on a horizontal attenuated total reflectance (HATR) accessory (Pike Industries). Electrochemical experiments were performed under a dinitrogen atmosphere using a BAS Epsilon EC-2000 potentiostat. Cyclic voltammetric data were taken at ambient temperature at 100 mV/s at 25 °C in a standard three-electrode cell from +1.7 to -1.7 V with a glassy carbon working electrode, *N,N*-dimethylacetamide (DMA) solvent, and tetrabutylammonium hexafluorophosphate (TBAH) electrolyte (~0.5 M). All potentials are reported versus NHE (normal hydrogen electrode) using cobaltocenium hexafluorophosphate ( $E_{1/2} = -0.78$  V) or ferrocene ( $E_{1/2} = 0.55$  V) as an internal standard. The peak-to-peak separation was less than 100 mV for all reversible couples. Elemental analyses (EA) were obtained from Atlantic Microlabs, Inc. Unless otherwise noted, all synthetic reactions and electrochemical experiments were performed under a dry nitrogen atmosphere.  $\text{CH}_2\text{Cl}_2$ , benzene, THF (tetrahydrofuran), and hexanes were purged with nitrogen and purified by passage through a column packed with activated alumina. Other solvents and liquid reagents were thoroughly purged with nitrogen prior to use. Deuterated solvents were used as received from Cambridge Isotopes. Compound **1** has been reported previously.<sup>27</sup>

**TpW(NO)(PMe<sub>3</sub>)(F)(Ph) (2).** A screw-cap vial was charged with **1**, TpW(NO)(PMe<sub>3</sub>)( $\eta^2$ -benzene) (500 mg, 0.863 mmol), then fluorobenzene (3.0 mL) was added. The mixture was capped and stirred at room temperature overnight. The reaction mixture was then added to 50 mL of pentane, and the precipitate was filtered, washed with pentane (10 mL  $\times$  3), and dried *in vacuo*. A light yellow solid (402 mg, 78% yield) was obtained. Crystals were grown from a  $\text{CDCl}_3$  and pentane solution, and an X-ray structure determination was carried out (details of the structural analysis are available in the Supporting Information).  $^1\text{H}$  NMR ( $\text{CDCl}_3$ , 300 MHz, 22 °C):  $\delta$  ppm 8.63 (dd,  $J = 5.9, 1.3$  Hz, 1H, H2), 8.11 (s, 1H, Tp), 7.85 (d,  $J = 2.0$  Hz, 1H, Tp), 7.63 (d,  $J = 1.5$  Hz, 1H, Tp), 7.54 (d,  $J = 2.0$  Hz, 1H, Tp), 7.48 (d,  $J = 2.0$  Hz, 1H, Tp),

7.43 (d,  $J = 1.5$  Hz, 1H, Tp), 7.25 (dd,  $J = 7.1, 7.1$  Hz, 1H, H3), 6.91 (dd,  $J = 7.08, 7.08$  Hz, 1H, H4), 6.73 (dd,  $J = 7.31, 7.31$  Hz, 1H, H5), 6.40 (t,  $J = 1.9, 1.9$  Hz, 1H, Tp), 6.33 (br d,  $J = 7.2$  Hz, 1H, H6), 6.22 (t,  $J = 1.9, 1.9$  Hz, 1H, Tp), 5.87 (t,  $J = 2.0, 2.0$  Hz, 1H, Tp), 1.34 (dd,  $J_{\text{P,H}} = 9.9, J_{\text{F,H}} = 1.3$  Hz, 9H, PMe<sub>3</sub>).  $^{13}\text{C}$  NMR ( $\text{CDCl}_3$ , 75 MHz, 25 °C):  $\delta$  ppm 183.2 (dd,  $J_{\text{F,C}} = 35.8, J_{\text{P,C}} = 10.7$  Hz, Ph C1), 144.6, 142.0, 141.3, 136.3 (1C each, Tp), 136.1 (d,  $J = 5.3$  Hz, Ph C2), 135.1 (Tp), 133.6 (d,  $J = 4.5$  Hz, Ph C6), 133.2 (Tp), 129.0 (d,  $J = 3.8$  Hz, Ph C3), 127.9 (d,  $J = 4.5$  Hz, Ph C5), 123.7 (d,  $J = 3.8$  Hz, Ph C4), 106.4, 105.8, 105.7 (1C each, Tp), 13.6 (dd,  $J_{\text{P,C}} = 28.3, J_{\text{F,C}} = 6.3$  Hz, PMe<sub>3</sub>).  $^{31}\text{P}$  NMR ( $\text{CDCl}_3$ , 121 MHz, 22 °C):  $\delta$  ppm 9.30 (d,  $J_{\text{F,P}} = 127.0, J_{\text{W,P}} = 212.5$  Hz).  $^{19}\text{F}$  NMR ( $\text{CDCl}_3$ , 282 MHz, 22 °C):  $\delta$  ppm -205.4 (d,  $J_{\text{P,F}} = 127.0$  Hz). FTIR (HATR glaze):  $\nu_{\text{NO}} = 1596$   $\text{cm}^{-1}$ . CV:  $E_{\text{p,a}} = -0.87$  V. Anal. Calcd for  $\text{C}_{18}\text{H}_{24}\text{BFN}_7\text{OPW}$ : C, 36.09; H, 4.04; N, 16.37. Found: C, 35.89; H, 3.98; N, 16.61.

**NMR Reaction of 2 with Et<sub>3</sub>SiH.** An NMR tube was charged with **2** (10 mg, 0.017 mmol) and  $\text{CDCl}_3$  (0.5 mL). Then  $\text{Et}_3\text{SiH}$  (16 mg, 0.138 mmol) was added. The tube was shaken briefly to effectively mix the compounds and then examined by NMR and GC-MS. Benzene:  $^1\text{H}$  NMR (300 MHz,  $\text{CDCl}_3$ , 22 °C):  $\delta$  ppm 7.34.  $\text{Et}_3\text{SiF}$ :  $^{19}\text{F}$  NMR (282 MHz,  $\text{CDCl}_3$ , 22 °C):  $\delta$  ppm -176.3 (sep,  $J = 6.2$  Hz) lit.,<sup>65</sup> EIMS  $m/z$  134 ( $\text{M}^+$ ), 105, 77 (100%), 63, 49, 47; the  $^1\text{H}$  NMR signals were overlapped by those from excess triethylsilane.

**NMR Reaction of 2 with PhMe<sub>2</sub>SiH.** An NMR tube was charged with **2** (10 mg, 0.017 mmol) and  $\text{CDCl}_3$  (0.5 mL), then  $\text{PhMe}_2\text{SiH}$  (15 mg, 0.110 mmol) was added. The tube was shaken briefly to effectively mix the compounds and then examined by NMR and GC-MS.  $\text{PhMe}_2\text{SiF}$ :  $^1\text{H}$  NMR (300 MHz,  $\text{CDCl}_3$ , 22 °C):  $\delta$  ppm 0.49 (d,  $J = 7.4$  Hz, 6H, Me), the  $^1\text{H}$  NMR signals of the phenyl group and free benzene were overlapped by those from excess phenyldimethylsilane.  $^{19}\text{F}$  NMR (282 MHz,  $\text{CDCl}_3$ , 22 °C):  $\delta$  ppm -162.1 (sep,  $J = 7.3$  Hz) lit.,<sup>66</sup> EIMS  $m/z$  154 ( $\text{M}^+$ ), 139 (100%), 121, 91, 77, 47.

**TpW(NO)(PMe<sub>3</sub>)( $\eta^2$ -Trifluoromethylbenzene) (3).** A screw-cap vial was charged with TpW(NO)(PMe<sub>3</sub>)( $\eta^2$ -benzene) (100 mg, 0.173 mmol), then trifluoromethylbenzene (0.8 mL) and pentane (0.8 mL) were added. The mixture was capped and stirred at room temperature overnight. Then pentane (10 mL) was added to the reaction mixture and the precipitate was filtered, washed with pentane (10 mL  $\times$  3), and dried *in vacuo*. A yellow solid was obtained (62 mg, 55% yield; two coordination diastereomers, **3A**: **3B** = 1.2:1).  $^1\text{H}$  NMR ( $\text{CDCl}_3$ , 300 MHz, 22 °C):  $\delta$  ppm 9.35 (d,  $J = 102.99$  Hz, 1H, W–H), 9.32 (d,  $J = 102.23$  Hz, 1H, W–H), 8.24 (d,  $J = 1.78$  Hz, 1H, Tp, minor), 8.11 (d,  $J = 1.81$  Hz, 1H, Tp, major), 7.88 (d,  $J = 1.82$  Hz, 2H, Tp, overlap), 7.77 (m, 4H, Tp, overlap), 7.67 (d,  $J = 1.7$  Hz, 2H, Tp, overlap), 7.50 (d,  $J = 6.7$  Hz, 1H, H2, major), 7.28 (d, 1H, H5, minor), 7.15 (br s, 2H, Tp, overlap), 7.13 (d, 1H, H2, minor), 6.87 (dd,  $J = 9.2, 5.2$  Hz, 1H, H5, major), 6.24 (m, 6H, Tp, overlap), 6.03 (dd,  $J = 9.3, 1.5$  Hz, 1H, H6 major), 5.94 (dd,  $J = 9.2, 1.14$  Hz, 1H, H6 minor), 3.95 (ddd,  $J = 12.9, 9.3, 5.3$  Hz, 1H, H4 major), 3.77 (br m, 1H, H3 minor), 2.43 (br dd, 1H, H4 minor), 2.30 (br dd, 1H, H3 major), 1.50 (d,  $J = 9.2$  Hz, 18H, PMe<sub>3</sub>'s of W–H compounds, overlap), 1.29 (d,  $J = 8.0$  Hz, 9H, PMe<sub>3</sub> minor), 1.28 (d,  $J = 8.0$  Hz, 9H, PMe<sub>3</sub> major).  $^{13}\text{C}$  NMR (acetone-*d*<sub>6</sub>, 75 MHz, 22 °C):  $\delta$  ppm 146.1 (2C), 143.3 (1C), 143.1 (1C), 142.7 (2C), 138.7 (2C), 138.1 (br m, 4C), Tp, some overlap, 138.0 (1C, Ph C2 major), 137.6 (1C, Ph C1 major), 137.5 (1C, Ph C1 minor), 137.2 (1C, Ph C2 minor), 135.8 (1C, Ph C5 minor), 135.5 (1C, Ph C5 major), 112.9 (1C, Ph C6 major), 111.3 (1C, Ph C6 minor), 108.1 (2C), 108.0 (2C), 107.6 (1C), 107.4 (1C), Tp, some overlap, 65.33 (d,  $J = 8.5$  Hz, 1C, Ph C4 major), 63.86 (1C, Ph C4 minor), 62.63 (d,  $J = 7.9$  Hz, 1C, Ph

(60) Kubas, G. J. In *Metal Dihydrogen and Sigma-Bond Complexes: Structure, Theory and Reactivity*; Kluwer: New York, 2001; Chapter 11.

(61) Delpech, F.; Sabo-Etienne, S.; Chaudret, B.; Daran, J.-C. *J. Am. Chem. Soc.* **1997**, *119*, 3167.

(62) Bart, S. C.; Lobkovsky, E.; Chirik, P. J. *J. Am. Chem. Soc.* **2004**, *126*, 13794.

(63) Luo, X. L.; Crabtree, R. H. *J. Am. Chem. Soc.* **1989**, *111*, 2527.

(64) Schubert, U.; Gilges, H. *Organometallics* **1996**, *15*, 2373.

(65) Adcock, W.; Binmore, G. T.; Krstic, A. R.; Walton, J. C.; Wilkie, J. J. *J. Am. Chem. Soc.* **1995**, *117*, 2758.

(66) Fujita, M.; Hiyama, T. *J. Org. Chem.* **1988**, *53*, 5405.

C3 minor), 61.19 (1C, Ph C3 major), 14.27 (d,  $J_{P,C} = 28.0$ ,  $\text{PMe}_3$ , overlap).  $^{31}\text{P}$  NMR ( $\text{CDCl}_3$ , 121 MHz, 25 °C):  $\delta$  ppm  $-2.69$ ,  $-2.83$  (both s, W–H compounds),  $-12.7$  ( $J_{W,P} = 306.9$  Hz, major),  $-13.8$  ( $J_{W,P} = 304.6$  Hz, minor).  $^{19}\text{F}$  NMR ( $\text{CDCl}_3$ , 282 MHz, 25 °C):  $\delta$  ppm  $-62.1$  (s, W–H compound),  $-62.9$  (s, major),  $-63.1$  (s, minor),  $-63.2$  (s, W–H compound). FTIR (HATR glaze):  $\nu_{\text{NO}} = 1575$   $\text{cm}^{-1}$ . CV:  $E_{\text{pa}} = 0.06$ ,  $0.42$  V. Anal. Calcd for  $\text{C}_{19}\text{H}_{24}\text{BF}_3\text{N}_7$ : OPW: C, 35.16; H, 3.73; N, 15.11. Found: C, 35.69; H, 3.87; N, 15.07.

**TpW(NO)(PMe<sub>3</sub>)(F)(3-PhCF<sub>3</sub>) (4).** A screw-cap vial was charged with TpW(NO)(PMe<sub>3</sub>)( $\eta^2$ -benzene) (300 mg, 0.516 mmol), then 3-fluoro-trifluoromethylbenzene (1.5 mL) and pentane (1.0 mL) were added. The mixture was capped and stirred at room temperature overnight. The reaction mixture was then added to 60 mL of pentane, and the precipitate was discarded. The filtrate was then concentrated to afford a brown solid (138 mg, 40% yield; two coordination diastereomers, **4A**:**4B** = 1.2:1).  $^1\text{H}$  NMR (300 MHz, acetone- $d_6$ , 22 °C):  $\delta$  ppm 8.90 (br s, 1H, A6), 8.81 (br d,  $J = 6.1$  Hz, 1H, B6), 8.12 (br s, 2H, Tp A&B), 8.02 (br s, 2H, Tp A&B), 7.90 (br s, 2H, Tp A&B), 7.77 (d,  $J = 2.0$  Hz, 2H, Tp A&B), 7.75 (d,  $J = 2.3$  Hz, 1H, Tp A), 7.73 (d,  $J = 2.2$  Hz, 1H, Tp B), 7.43 (dd,  $J = 7.5$ ,  $7.5$  Hz, 1H, B5), 7.40 (d,  $J = 1.5$  Hz, 1H, Tp A), 7.37 (d,  $J = 1.9$  Hz, 1H, Tp B), 7.21 (br s, 2H, A4, B4), 6.89 (dd,  $J = 7.6$ ,  $7.6$  Hz, 1H, A3), 6.67 (br s, 1H, A2), 6.65 (br s, 1H, B2), 6.51 (m, 2H, Tp A&B), 6.28 (t,  $J = 2.1$ ,  $2.1$  Hz, 2H, Tp A&B), 6.00 (t,  $J = 2.2$ ,  $2.2$  Hz, 1H, Tp A), 5.97 (t,  $J = 2.2$ ,  $2.2$  Hz, 1H, Tp B), 1.36 (d,  $J_{P,H} = 10.2$  Hz, 9H, B  $\text{PMe}_3$ ), 1.35 (d,  $J_{P,H} = 10.2$  Hz, 9H, A  $\text{PMe}_3$ ).  $^{13}\text{C}$  NMR (75 MHz, acetone- $d_6$ , 22 °C):  $\delta$  ppm 185.4 (dd,  $J_{F,C} = 35.5$  Hz,  $J_{P,C} = 11.0$  Hz, A1), 185.3 (dd,  $J_{F,C} = 35.3$  Hz,  $J_{P,C} = 9.9$  Hz, B1), 145 (Tp B), 145.7 (Tp A), 144.9 (Tp A), 144.9 (Tp B), 143.2 (Tp A&B), 141.4 (d,  $J = 4.5$  Hz, B2), 139.3 (A6), 138.8 (Tp A&B), 137.9 (Tp A), 137.8 (Tp B), 135.5 (Tp A&B), 134.0 (B6), 131.7 (A2), 130.7 (d,  $J = 3.8$  Hz, B5), 129.6 (d,  $J = 4.5$  Hz, A5), 121.8 (m, A4 & B4), 108.6 (Tp A&B), 108.0 (Tp A), 107.9 (Tp B), 107.2 (Tp A&B), 14.6 (d,  $J = 6.7$  Hz,  $\text{PMe}_3$  B), 14.2 (d,  $J = 6.7$  Hz,  $\text{PMe}_3$  A).  $^{19}\text{F}$  NMR (282 MHz, acetone- $d_6$ , 22 °C):  $\delta$  ppm  $-63.0$  (s,  $\text{CF}_3$ , A),  $-63.5$  (s,  $\text{CF}_3$ , B),  $-195.2$  (d,  $J_{P,F} = 124.1$  Hz, W–F, A),  $-195.6$  (d,  $J_{P,F} = 123.6$  Hz, W–F, B).  $^{31}\text{P}$  NMR (121 MHz, acetone- $d_6$ , 22 °C):  $\delta$  ppm  $-9.4$  (d,  $J_{F,P} = 125.3$  Hz,  $J_{W,P} = 210.8$  Hz, A),  $-8.8$  (d,  $J_{F,P} = 124.6$  Hz,  $J_{W,P} = 207.6$  Hz, B). IR (HATR glaze):  $\nu_{\text{NO}} = 1600$   $\text{cm}^{-1}$ . CV (DMA, TBAH, 100 mV/s, vs NHE):  $E_{\text{pa}} = -0.75$  V.

**TpW(NO)(PMe<sub>3</sub>)( $\eta^2$ -C<sub>6</sub>F<sub>6</sub>) (5).** A screw-cap vial was charged with TpW(NO)(PMe<sub>3</sub>)( $\eta^2$ -benzene) (100 mg, 0.172 mmol), then hexafluorobenzene (1.0 mL) and pentane (1.5 mL) were added. The mixture was capped and stirred at room temperature overnight. The reaction mixture was then added to 60 mL of pentane, and the precipitate was filtered, washed with pentane (10 mL  $\times$  3), and dried *in vacuo*. A yellow solid (55 mg, 46% yield) was obtained. Attempts to purify this solid were thwarted by its unstable nature in solution.  $^1\text{H}$  NMR (acetone- $d_6$ , 300 MHz, 22 °C):  $\delta$  ppm 8.11 (d, 1H,  $J = 2.0$  Hz, Tp), 8.05 (br s, 3H, Tp), 7.92 (d, 1H,  $J = 2.2$  Hz, Tp), 7.86 (br s, 1H, Tp), 6.48 (t, 1H,  $J = 2.1$  Hz, Tp), 6.37 (m, 2H, Tp), 1.29 (d, 1H,  $J_{P,H} = 9.3$  Hz,  $\text{PMe}_3$ ).  $^{13}\text{C}$  NMR (acetone- $d_6$ , 75 MHz, 22 °C):  $\delta$  ppm 146.4, 146.2, 145.8, 145.7, 139.1, 138.7 (Tp 3,5 and Ph), 109.2, 107.9, 107.8 (Tp 4), 80.2 (bound Ph), 14.8 (d, 3C,  $J = 30.0$  Hz,  $\text{PMe}_3$ ).  $^{13}\text{C}$  NMR signals were very weak due to its poor stability in solution.  $^{19}\text{F}$  NMR (acetone- $d_6$ , 282 MHz, 22 °C):  $\delta$  ppm  $-144.8$  (td,  $J = 51.7$ ,  $16.9$ ,  $16.9$  Hz),  $-147.3$  (ddt,  $J = 41.5$ ,  $18.9$ ,  $18.8$ ,  $14.6$  Hz),  $-169.2$  (td,  $J = 39.6$ ,  $19.9$ ,  $19.9$  Hz),  $-178.6$  (br t,  $J = 15.3$ ,  $15.3$  Hz),  $-181.5$  (ddd,  $J = 17.6$ ,  $9.3$ ,  $4.1$  Hz),  $-187.3$  (ddd,  $J = 19.0$ ,  $16.9$ ,  $9.9$  Hz).  $^{31}\text{P}$  NMR (121 MHz, acetone- $d_6$ , 22 °C):  $\delta$  ppm  $-11.1$  (d,  $J_{F,P} = 4.1$  Hz,  $J_{W,P} = 255.9$  Hz). IR (HATR glaze):  $\nu_{\text{NO}} = 1616$   $\text{cm}^{-1}$ . CV (DMA, TBAH, 100 mV/s, vs NHE):  $E_{\text{pa}} = -0.19$  V.

**TpW(NO)(PMe<sub>3</sub>)( $\eta^2$ -1-fluoronaphthalene) (6).** A screw-cap vial was charged with TpW(NO)(PMe<sub>3</sub>)( $\eta^2$ -benzene) (100 mg, 0.172 mmol), then 1-fluoronaphthalene (740 mg) and pentane (1.0 mL) were added. The mixture was capped and stirred at room temperature overnight. The reaction mixture was then added to 60 mL of pentane, and the precipitate was filtered, washed with pentane (10 mL  $\times$  3), and dried *in vacuo*. A red solid (77 mg, 69% yield) was obtained. Four coordination diastereomers in ca. 1:1:1:1 ratio were obtained; only selected NMR signals are reported here.  $^1\text{H}$  NMR (300 MHz, acetone- $d_6$ , 22 °C):  $\delta$  ppm 6.56 (dd,  $J = 14.52$ ,  $5.29$  Hz, 1H, A2), 6.44 (d,  $J = 7.6$  Hz, 1H, B4), 3.81 (m, 3H, D7, C6, A3), 3.60 (ddd,  $J = 29.67$ ,  $11.02$ ,  $5.45$  Hz, 1H, B2), 2.64 (d,  $J = 9.1$  Hz, 1H, D8), 2.35 (d,  $J = 9.27$  Hz, 1H, C5), 2.25 (d,  $J = 9.5$  Hz, 1H, A4), 1.38 (d,  $J = 3.03$  Hz, 3H,  $\text{PMe}_3$ ), 1.35 (d,  $J = 3.2$  Hz, 3H,  $\text{PMe}_3$ ), 1.34 (d,  $J = 2.9$  Hz, 3H,  $\text{PMe}_3$ ), 1.32 (d,  $J = 3.05$  Hz, 3H,  $\text{PMe}_3$ ).  $^{13}\text{C}$  NMR (75 MHz, acetone- $d_6$ , 22 °C):  $\delta$  ppm 59.6, 58.5, 58.4, 58.3, 58.3, 58.1, 55.1, 53.3 (bound), 13.5 (d,  $J = 27.7$  Hz,  $\text{PMe}_3$ ), 13.3 (d,  $J = 27.5$  Hz,  $\text{PMe}_3$ ), 13.2 (d,  $J = 27.4$  Hz,  $\text{PMe}_3$ ).  $^{19}\text{F}$  NMR (282 MHz, acetone- $d_6$ , 22 °C):  $\delta$  ppm  $-125.4$  (br m),  $-127.6$  (dd,  $J = 10.3$ ,  $5.9$  Hz),  $-141.8$  (br d,  $J = 12.6$  Hz),  $-151.0$  (br d,  $J = 30.2$  Hz).  $^{31}\text{P}$  NMR (121 MHz, acetone- $d_6$ , 22 °C):  $\delta$  ppm  $-12.3$ ,  $-12.8(7)$ ,  $-12.9$ ,  $-14.6$ . IR (HATR glaze):  $\nu_{\text{NO}} = 1573$   $\text{cm}^{-1}$  (mixture of isomers). CV (DMA, TBAH, 100 mV/s, vs NHE):  $E_{\text{pa}} = +0.54$  V (mixture of isomers).

**TpW(NO)(PMe<sub>3</sub>)(HSi(Et)<sub>3</sub>) (9).** A screw-cap vial was charged with TpW(NO)(PMe<sub>3</sub>)( $\eta^2$ -benzene) (300 mg, 0.516 mmol), then triethylsilane (0.5 mL) and THF (2.0 mL) were added. The mixture was capped and stirred at room temperature overnight. The reaction mixture was then added to 50 mL of pentane, and the precipitate was filtered and discarded. The filtrate was then concentrated *in vacuo* to afford a brown solid (158 mg, 49% yield).  $^1\text{H}$  NMR (acetone- $d_6$ , 300 MHz, 22 °C):  $\delta$  ppm 8.02 (d, 1H,  $J = 1.9$  Hz, Tp), 7.96 (d, 1H,  $J = 1.9$  Hz, Tp), 7.85 (d, 1H,  $J = 2.3$  Hz, Tp), 7.85 (d, 1H,  $J = 2.3$  Hz, Tp), 7.79 (d, 1H,  $J = 2.4$  Hz, Tp), 7.75 (d, 1H,  $J = 2.0$  Hz, Tp), 6.30–6.26 (m, 3H, Tp 4), 3.85 (d, 1H,  $J_{P,H} = 64.2$  Hz,  $J_{W,H} = 39.6$  Hz, Si–H), 1.56 (d, 9H,  $J_{P,H} = 8.6$  Hz,  $\text{PMe}_3$ ), 1.00–0.53 (m, 15H, Et<sub>3</sub>).  $^{13}\text{C}$  NMR (acetone- $d_6$ , 75 MHz, 22 °C):  $\delta$  ppm 146.4, 146.2, 145.9, 138.0, 137.6, 137.5 (1C each, Tp 3,5), 107.4 (1C), 107.3 (2C, Tp 4), 19.1 (d, 3C,  $J = 30.3$  Hz,  $\text{PMe}_3$ ), 12.1 (3C, CH<sub>2</sub>), 10.1 (3C, CH<sub>3</sub>).  $^{31}\text{P}$  NMR (acetone- $d_6$ , 121 MHz, 22 °C):  $\delta$  ppm  $-11.36$  (d,  $J_{W,P} = 242.9$  Hz). IR (HATR glaze):  $\nu_{\text{NO}} = 1566$   $\text{cm}^{-1}$ . CV (DMA, TBAH, 100 mV/s, vs NHE):  $E_{\text{pa}} = +0.34$  V. Two attempts to analyze a sample with HRMS (ESI<sup>+</sup>) were unsuccessful.

**TpW(NO)(PMe<sub>3</sub>)(HSi(Me)<sub>2</sub>(Ph)) (10).** A screw-cap vial was charged with TpW(NO)(PMe<sub>3</sub>)( $\eta^2$ -benzene) (200 mg, 0.344 mmol), then dimethylphenylsilane (0.5 mL) and THF (0.5 mL) were added. The mixture was capped and stirred at room temperature overnight. The reaction mixture was then added to 50 mL of pentane, and the precipitate was filtered and discarded. The filtrate was then concentrated *in vacuo* to afford a brown solid (121 mg, 55% yield).  $^1\text{H}$  NMR (acetone- $d_6$ , 300 MHz, 22 °C):  $\delta$  ppm 8.04 (d, 1H,  $J = 2.0$  Hz, Tp), 7.89 (d, 1H,  $J = 2.3$  Hz, Tp), 7.85 (d, 1H,  $J = 2.3$  Hz, Tp), 7.72 (d, 1H,  $J = 2.4$  Hz, Tp), 7.52 (d, 1H,  $J = 1.9$  Hz, Tp), 7.46 (d, 1H,  $J = 2.0$  Hz, Tp), 7.35–7.31 (m, 2H, Ph), 7.19–7.07 (m, 3H, Ph), 6.29 (t, 1H,  $J = 2.2$  Hz, Tp), 6.21 (t, 1H,  $J = 2.2$  Hz, Tp), 6.03 (t, 1H,  $J = 2.2$  Hz, Tp), 4.31 (d, 1H,  $J_{P,H} = 66.4$  Hz,  $J_{W,H} = 38.1$  Hz, Si–H), 1.51 (d, 1H,  $J = 8.8$  Hz,  $\text{PMe}_3$ ), 0.32 (s, 1H, CH<sub>3</sub>), 0.23 (s, 1H, CH<sub>3</sub>).  $^{13}\text{C}$  NMR (acetone- $d_6$ , 75 MHz, 22 °C):  $\delta$  ppm 154.3 (1C, Ph), 146.4, 146.3, 146.2, 138.0, 137.8, 137.5 (1C each, Tp 3,5), 135.5 (2C, Ph), 128.6 (2C, Ph), 128.0 (1C, Ph), 107.4, 107.2, 107.0 (1C each, Tp 4), 19.1 (d, 3C,  $J = 30.6$  Hz,  $\text{PMe}_3$ ), 6.7 (Me), 5.7 (Me).  $^{31}\text{P}$  NMR (acetone- $d_6$ , 121 MHz, 22 °C):  $\delta$  ppm  $-10.59$  (d,  $J_{W,P} = 241.8$  Hz). IR (HATR glaze):  $\nu_{\text{NO}} = 1569$   $\text{cm}^{-1}$ . LRMS (direct inlet): 636, 637, 638, 639(max), 640, 641, 642.



**Acknowledgment.** This work was supported by the NSF (CHE-0111558, 9974875, and 0116492 (UR)).

**Supporting Information Available:** Full synthetic details for the preparation of compounds **2–6**, **9**, and **10** and spectra, as well

as the cif file for the structure of **2**, and the full ref 42. This material is available free of charge via the Internet at <http://pubs.acs.org>.

OM070099J